Spatial Variability and Liquefaction in Reclaimed Sites

Ahmad Kahiel
American University of Beirut, Beirut, Lebanon, amk77@mail.aub.edu

Salah Sadek[1], Shadi Najjar[2]
American University of Beirut, Beirut, Lebanon, salah@aub.edu.lb [1], sn06@aub.edu.lb[2]

ABSTRACT: The reliable characterization of spatial variability is vital for obtaining dependable and well-founded estimates of soil properties. The spatial correlation structure is inherently related to the dependability of underlying source data. In typical site investigation programs and due to economical limitations, the distribution of the boreholes across the site results in data points that are closely spaced in the vertical direction (sampling interval) while larger spacing are obtained in the horizontal direction (borehole density across the site). This poses a problem when generating the 3-Dimensional variogram since the contribution of the horizontally spaced data points to the small lag distances (less the 15m) is typically null. A case study of a reclaimed site that was investigated with an array of boreholes is considered. The spatial correlation structure of the SPT blows across the site is characterized assuming isotropic soil properties. The validity of this assumption is tested using another set of localized and concentrated boreholes within the site. Conditioned spatially variable random fields were generated and utilized in developing liquefaction potential maps. Additional boreholes were added to a previously performed study to get a more reliable characterization of the site of interest.

Keywords: spatial variability; reclaimed sites; liquefaction.

1. Introduction

The loss of strength of loose cohesionless soils during seismic events is one of the major causes of damage after earthquakes. This strength loss is attributed to the accumulation of pore water pressure leading to a reduction in the effective stress and a decrease in the shear strength of the soil. The occurrence of liquefaction is usually associated with surface manifestations such as sand boils, differential settlement, and lateral spreading (B. Seed & Lee, 1966; Terzaghi, Peck, & Mesri, 1996). Although early studies related to this phenomenon date back to more than 50 years, it is still a major field of study and research to date. Several case histories reported liquefaction in reclaimed sites. Examples of these are the Kaikoura earthquake (Mw = 7.8) which led to massive damage to CentrePort of Wellington as a result of the liquefaction of the reclaimed supporting soil (Cubrinovski et al., 2017; Cubrinovski et al., 2018). Liquefaction was also noticed in a reclaimed site in Taiwan after the 1999 Chi-Chi earthquake (Yu, Shieh, & Chung, 2000). Tanaka (1996) presented liquefaction damage caused by the 1995 Hanshin earthquake in the reclaimed lands along the north shore of Osaka bay. On the other hand, reclaimed sites that were partially improved were valuable cases to investigate. A comparison of cone penetration results pre and post dynamic compaction performed to a reclaimed site showed that the liquefaction susceptibility decreased substantially due to the improvement adopted (Ku & Juang, 2011; Shen, Martin, Ku, & Lu, 2018). Increased strength and reduced variability was the major finding of these studies. A magnitude 9 earthquake in Japan caused liquefaction in unimproved zones while areas treated with sand compaction piles didn't liquefy (Yasuda, Harada, Ishikawa, & Kanemaru, 2012). Cubrinovski, Ishihara, & Furukawazono (2000) discussed two case histories on liquefaction of reclaimed sites (densified and undensified) after the 1995 Kobe earthquake. Lower settlement was reported for the densified site as compared to the undensified one. It is worthy to note that none of these authors aimed at characterizing the spatial variability of soil properties across the reclaimed areas.

Many approaches were developed to assess the susceptibility of soils to liquefaction (Andrus & Stokoe II, 2000; Idriss & Boulanger, 2008; Robertson & Wride, 1998; H. B. Seed & Idriss, 1971; Youd & Idriss, 2001) These studies are empirical and correlated the occurrence of liquefaction with field test indices such as standard penetration test (SPT), cone penetration test (CPT) and shear wave velocity (vs). Additionally, different indices were calibrated with the occurrence of surficial manifestations of liquefaction. The Liquefaction Potential Index (LPI) developed by Iwasaki et al. (1978) integrates the "unsafe" locations (FS<1) in a borehole with a linearly decreasing weight up to depths of 20m. Other indices such as one-dimensional post-liquefaction reconsolidation settlement, liquefaction severity number, and the Ishihara inspired liquefaction potential index were also proposed and adopted.

These indices are useful when combined with geostatistical tools to develop liquefaction hazard maps. Pokhrel, Kuwano, & Tachibana (2013) used data from 86 boreholes in Saitama City, Japan (217.5 Km2) to krige liquefaction indices for seismic hazard assessment. They validated their model with a second set of 41 boreholes. Li, Wang, & Yuan (2014) used 65 boreholes to generate a liquefaction zoning map of south Tangshan. Al-Ani, Oh, Chai, & Al-Uzairy (2014) developed zonation maps for SPT-N values using the IDW interpolation method in Paradise Australia (4.2 Km2 with data collected from 35 locations). Sun (2012) constructed seismic zoning maps using site period and vs data for liquefaction mitigation in Gyeongju.

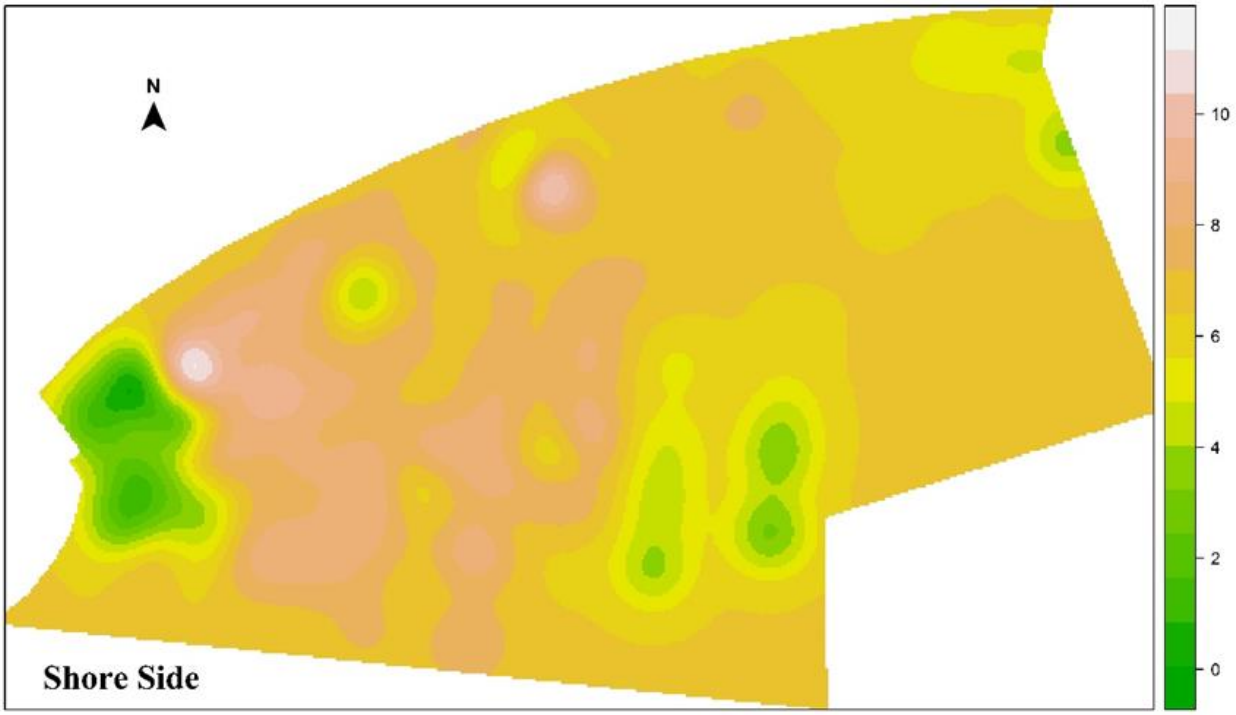

Figure 1. Digital elevation model of the site (MSL, m).

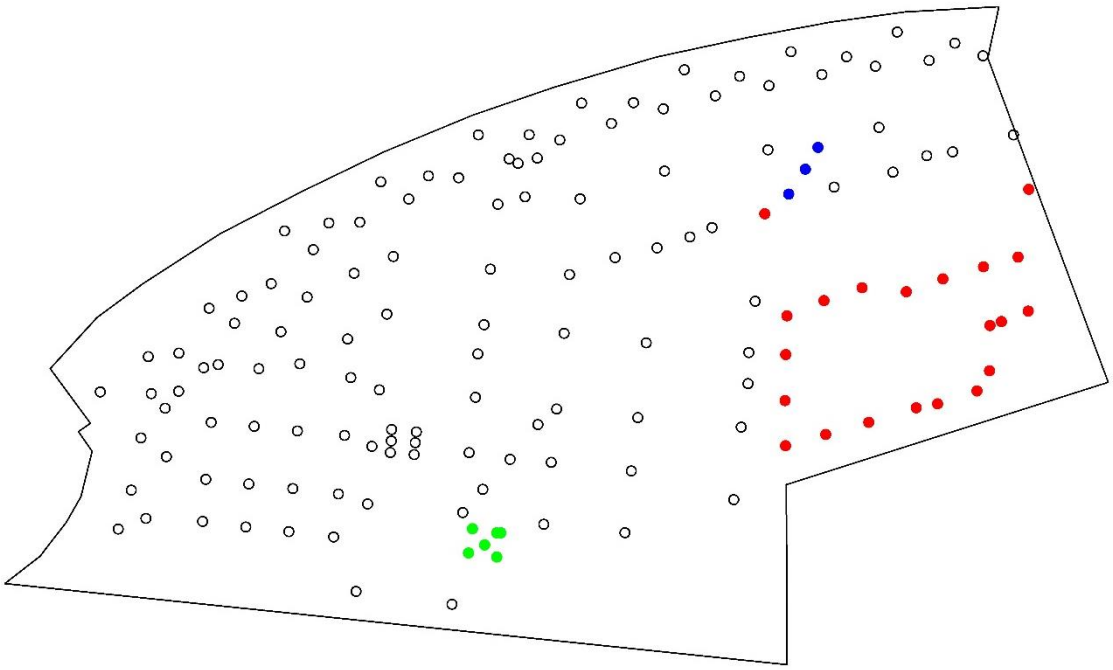

Figure 2. Location of boreholes across the site.

Additionally, the assessment of spatial variability is useful for design refinement considerations. For example, Bong & Stuedlein (2018) characterized the vertical and horizontal spatial variability of a site and utilized the generated random fields for predicting the differential settlement for a given earthquake event. Conditioning spatial variability with available field data results in more representative random fields of reality (Baker and Faber 2008). Random field theory was successfully incorporated within finite element analyses. Popescu, Prevost, & Deodatis (2004) and Popescu, Prévost, & Deodatis (1997) performed 2- and 3-dimensional non-linear dynamic analyses for Monte-Carlo-simulated random fields. Effects of soil susceptibility to liquefaction and seismic excitation frequency content were investigated. Results showed that 2-D analysis acceptably predicts soil liquefaction but not differential settlements. A minor effect for the horizontal scale of fluctuation on the amount of earthquake induced pore water pressure was observed.

Average soil properties used in deterministic analyses result in less pore water pressure as compared to stochastic analyses. Fenton & Vanmarcke (1998) performed 1-D non-linear finite element analyses incorporating spatial variability for a site that liquefied after an earthquake. Results showed that only 20% of the site will liquefy in contradiction with actual performance. To explain this discrepancy, the authors suggested that even this little percentage of liquefaction at the site may trigger larger lateral spreading. The spatial variability of mildly sloping grounds with top nonliquefiable crust was modeled in 3D non-linear finite element analysis (Montgomery & Boulanger, 2016). Characteristic design values for a deterministic analysis that results in comparable output to that of the simulation were identified. It was noticed that as the crust thickness increases, differential settlement was noticeably decreased. Kahiel et al. 2019 characterized the spatial variability of a reclaimed site. Liquefaction potentail maps were developed for the site. In their study the data was distributed across the site such that the horizotal spacing beteween the boreholes is much larger than that in the vertical direction. This resulted in a variograms that is governed by the vertically spaced data pairs particularly at small lag distances (<12m).

In this paper, additional boreholes to the previous study are utilized to characterize spatial variability and develop liquefaction hazard maps for the reclaimed area in Lebanon using an array of SPT data for different seismic scenarios. The 3-dimensional variogram representing the variability and the correlation structure of the SPT data was determined and used to krige the data across the site. The kriged data was then used in the Idriss & Boulanger (2008) liquefaction triggering procedure to compute the means and variances of the factors of safety against liquefaction across the site. These factors of safety were then combined with the Iwasaki approach to estimate the liquefaction vulnerability.

2. Site characterization

The site of interest which is adopted as a test case covers a total area of approximately half a square kilometer. The area was reclaimed after it was initially used as an un-engineered dump for two decades. Inert land excavation products and construction wastes were mainly used in the reclamation process. The ground level is generally assumed to be relatively flat ranging from +2m to +8m MSL. Figure 1 shows a digital elevation model of the site. SPT data from 146 boreholes collected at 1.5m depth intervals were collected as part of a site investigation program. The boreholes covered the totality of the site with spacing varying from 12 to 100m at most (figure 2). Figure 2 shows the distribution of the boreholes across the site. Colored circles are the new data inculded in this study. The total soil profile thickness (until bedrock) increases from 7m to 34m as one moves away from the shore. The investigation showed that the fill can be characterized as highly variable loose granular material underlain by a native seabed sand layer of variable thickness ranging from 0.5m up to 8m overlying marly rock. The water table was taken to be at sea level as confirmed by piezometer readings.

SPT values ranged from a minimum of 3 up to 70 with an overall mean value of about 18 and a coefficient of variation (COV) of 0.74 (total variability). A histogram representation of the SPT data (Fig. 3) indicates that the data follows a lognormal distribution. Most of the retrieved samples had fines content (FC) ranging from zero (clean sand) up to 35% with a small number of extreme values (above 60%) in some pockets as shown in Figure 4.

3. Methodology

The procedure may be divided into three main parts: Characterizing spatial variability in soil parameters (N and FC), calculating the factor of safety against liquefaction, and lumping factors of safety at each soil column into a single representative value (LPI) or calculating the exposed length of piles. More details are provided in the following subsections.

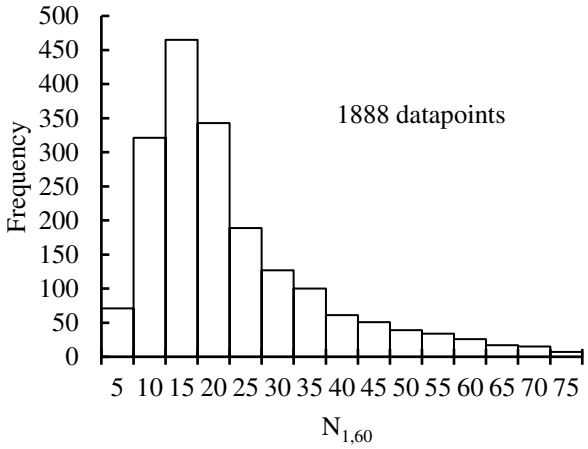

Figure 3. Histogram of $(N_1)_{60}$ across the site.

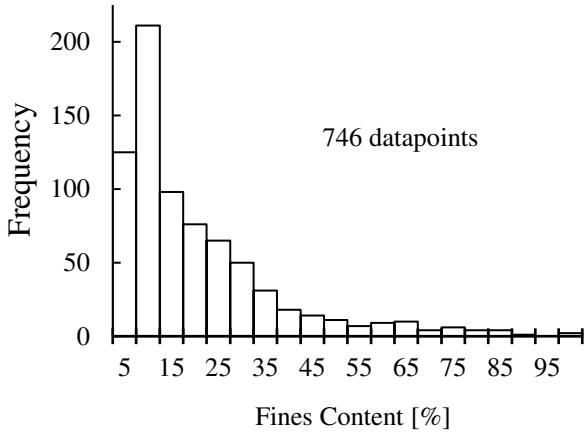

Figure 4. Histogram of fines content across the site.

3.1. Spatial variability model

In natural soil/rock sites, horizontal and vertical scales of fluctuation need to be specified in order to model the spatial variability of a given soil property. These scales of fluctuation are a byproduct of the depositional processes that took place during the formation of the soil layer. In reclaimed lands where the

fill is formed by dumping soils by trucks and barges, it is likely that the soil properties will exhibit an isotropic correlation structure. An isotropic correlation structure is supported by an initial assessment of the lateral and vertical semi-variograms for lag distances in which both lateral and vertical data is available (greater than 14m). Based on the above, it was assumed that the 3-dimensional semi-variogram is a suitable representation of the spatial variability of the reclaimed site. Extensive data collection was performed to further support this assumption; however, few boreholes had a horizontal separtion distance below 10m.

As a first step, $(N_1)_{60}$ was obtained from the given SPT data by correcting for overburden pressure and energy. The former correction is important because it adjusts the increasing trend in the SPT values along the vertical direction. Since these parameters were lognormally distributed, the natural log (LN) of each was obtained to meet the normality criterion for the kriging. The 3-dimensional experimental semi-variogram (omnidirectional) for each parameter was generated and fitted with an exponential theoretical variogram as shown in Figures 5 and 6, respectively. However it should be noted here that due to the fact that the sampling spacing in the vertical direction (minimum of 1.5m) is much smaller than that in the horizontal direction (minimum of 15m), the points of the variograms corresponding to low lag distances (less than 14m) will be governed by the vertically spaced data points. This is manifested by the overlap of the variogram points below 14m lag distance. While for lag distances above 14m we can notice variations between the directional variogram as a result of the contribution of the horizontal pairs of the data points. Nonetheless, this variation is minimal and the 3D omnidirectional variogram is adopted in further analysis. The LN(FC) and LN($(N_1)_{60}$) variograms have nuggets of 0.12 and 0.17 respectively. These values are equivalent to half of the variance corresponding to the measurement error. For the SPT, the nugget value corresponds to a COV due to measurement error of 0.63 which falls in line with ranges provided by (Kulhawy & Trautmann, 1996; Phoon & Kulhawy, 1999a; Phoon & Kulhawy, 1999b). This very high measurement error implies that even if the location of the unsampled point was close to the borehole sampled data, it is possible to have dissimilar values. This effect emerges from measurement errors, small scale variability or as a result of model fitting since no data are available for lag distances less than 1.5m.

Next, ordinary kriging was used to estimate LN($(N_1)_{60}$) and LN(FC) at unsampled locations on a 3-dimensional grid having 3m by 3m spacing in the horizontal direction and a 1m-spacing in the vertical direction. The generated random fields are back-transformed and at each node ($(N_1)_{60}$ and FC), the equivalent clean sand SPT maps $(N_1)_{60,cs}$ were then obtained for use as input to the Idriss and Boulanger (2008) liquefaction assessment procedure. It is worthy to note that the kriging process results in map of the expected values of the parameter of interest (i.e $(N_1)_{60}$ and FC) and the associatied variance at each location. In this paper the liquefaction anaylsis is performed based on the expected values without the incorporation of the variance which will adopted in the extended furure research. The model uncertainty of the liquefaction-triggering equation as well as the uncertainty in the stress reduction factor, total and effective stresses were neglected (Christian & Baecher, 2016).

3.2. Liquefaction assessment

The SPT-based liquefaction analysis procedure presented in Idriss and Boulanger (2008) was adopted in the liquefaction assessment. At every node in the 3-D grid, the factor of safety against liquefaction was calculated as the ratio of the CRR to the CSR. The CSR was calculated for a range of earthquake magnitudes covering wide recurrence periods (50 to 1000 years) and different peak ground accelerations.

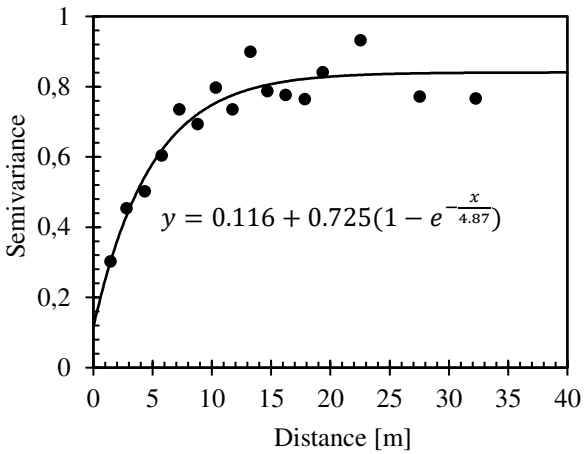

Figure 5. Experimental and theoretical semi-variograms for natural logarithm of the fines content.

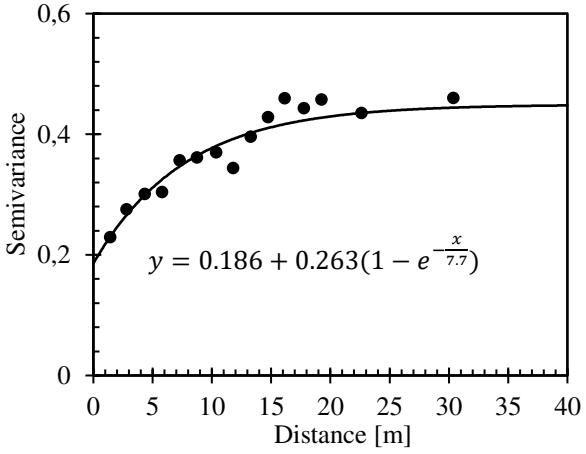

Figure 6. Experimental and theoretical semi-variograms for the natural logarithm of $(N_1)_{60}$.

3.3. Liquefaction potential index

Given the maps of the factors of safety produced, the LPI was then calculated by lumping the top vertical 20m strip of factors of safety at every node in a single value. LPI was defined in Iwasaki et al. (1978) using the following equation:

$$LPI = \int_0^{20} F \cdot w \cdot dz \quad (1)$$

Where F=1-FS when FS<1, F=0 when FS>1, w=10-z/2. The map showing the variation of the liquefaction

potential index along the site are plotted in Figure 7 for earthquake magnitudes of 7.25 with a peak ground acceleration of 0.25g. In these figures, LPI values less than 5 represent low risk of liquefaction, values between 5 and 10 represent intermediate potential for liquefaction, and values larger than 15 reflect high liquefaction susceptibility. These plots show the significance of the earthquake magnitude on the degree of liquefaction across the site. It is generally noticed that peripheral zones (east, west, and north) in the site are the weakest while central areas with a thinner soil layer (south, near shore) show lower liquefaction susceptibility.

4. Analysis and discussion

Figure 7 indicates that the liquefaction potential index is dependent on three main factors. The first factor is the soil cyclic resistance compared to the cyclic demand characterized by the factor of safety across the soil column. The second factor is the proximity of the liquefiable layer to the surface. Areas where the soil layer above the water table is thinner resulted in higher LPI as compared to areas with thicker dry top layer. These areas, which appear in green in Figure 1, had the highest LPI values across the site. This observation is similar to that presented in Montgomery & Boulanger (2016) for slopes with non-liquefiable crust on top. A similar note was presented by Bray & Dashti (2014) by comparing free field and under buildings generation of pore water pressure. This was attributed to the reduced shear-induced displacements. The third factor is the thickness of the liquefiable layer. As the liquefiable layer thickness increases, the liquefaction potential index increases and vice versa. This is recognized in the low LPI values in the south zone of the site and the high LPI values in the northern area. This might be attributed to the decreasing weight with depth used in the calculation of the LPI.

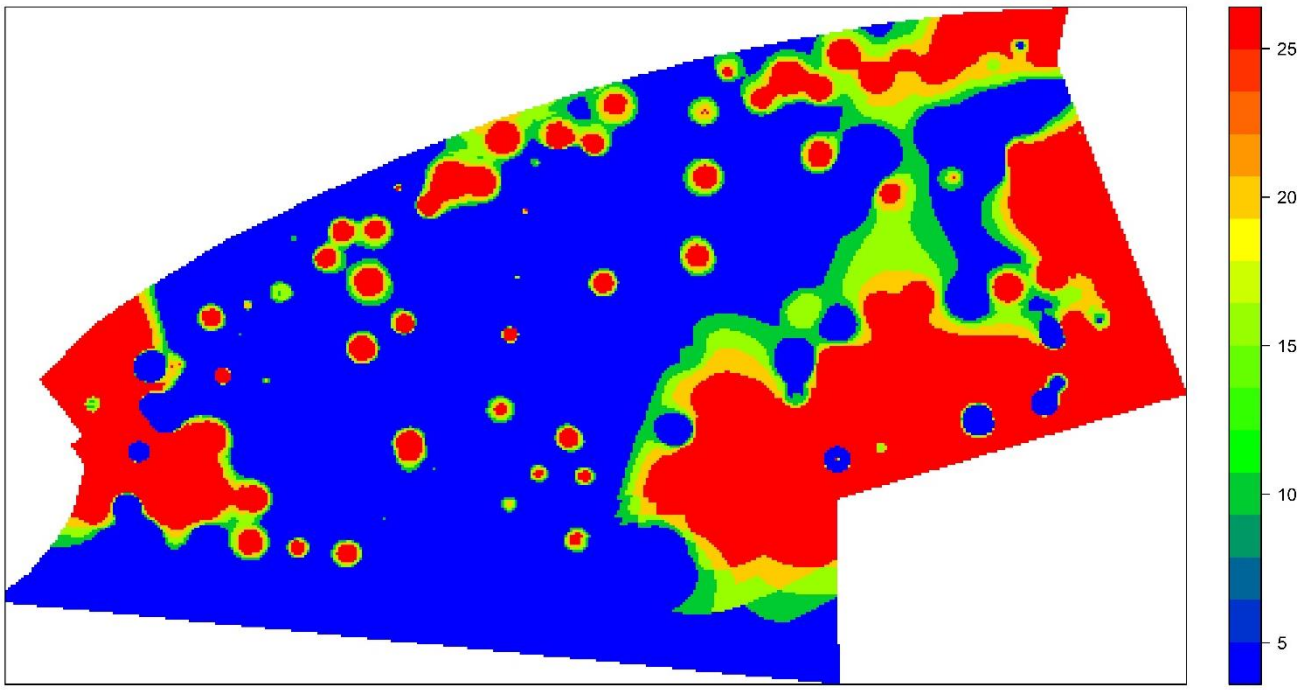

Figure 7. Liquefaction Potential Index maps for earthquake magnitudes of 7.25 (top)– a_{max}= 0.25g.

5. Conclusion

This paper presented a procedure for the development of a liquefaction hazard map in reclaimed lands. Unlike conventional soil profiles that are characterized by vertical and horizontal correlation lengths that are different, the spatial varaibility of the standard penertration test blowcounts in the site was characterized by an isotropic three-dimensional semivariogram. Maps of factors of safety were then generated and used to produce liquefaction potential index maps for the site. These maps will allow engineers to make informed decisons with regards to potential rehabilitation or improvement measures to be taken at the site. It is important to note that the case used to illustrate the methodology presented relied on actual data, with seismic events selected to produce interesting levels of liquefaction which allowed for an appreciation of the usefullness of the technique. The goal is to show that engineers can benefit from the approach presented in guiding ground improvement decisions/designs.

References

[1] Al-Ani, H., Oh, E., Chai, G., & Al-Uzairy, B. N. (2014). GIS-interpolated geotechnical zonation maps in surfers paradise, australia. 6th International Conference on Advanced Geographic Information Systems, Applications, and Services (GEO-Processing 2014), Spain, Barcelona, , 142 148.

[2] Andrus, R. D., & Stokoe II, K. H. (2000). Liquefaction resistance of soils from shear-wave velocity. Journal of Geotechnical and Geoenvironmental Engineering, 126(11), 1015-1025.

[3] Bong, T., & Stuedlein, A. W. (2018). Effect of cone penetration conditioning on random field model parameters and impact of spatial variability on liquefaction-induced differential settlements. Journal of Geotechnical and Geoenvironmental Engineering, 144(5), 04018018.

[4] Bray, J. D., & Dashti, S. (2014). Liquefaction-induced building movements. Bulletin of Earthquake Engineering, 12(3), 1129-1156.
[5] Christian, J. T., & Baecher, G. B. (2016). Sources of uncertainty in liquefaction triggering procedures. Georisk: Assessment and Management of Risk for Engineered Systems and Geohazards, 10(4), 242-250.
[6] Cubrinovski, M., Bray, J., de la Torre, C., Olsen, 4. M., Bradley, B., Chiaro, G., Stock, E., & Wotherspoon, L. (2017). Liquefaction effects and associated damages observed at the wellington CentrePort from the 2016 kaikoura earthquake.
[7] Cubrinovski, M., Bray, J. D., de la Torre, C., Olsen, M., Bradley, B., Chiaro, G., Stocks, L., Wotherspoon, L., & Krall, T. (2018). Liquefaction-induced damage and CPT characterization of the reclamations at CentrePort, wellington. Bulletin of the Seismological Society of America,
[8] Cubrinovski, M., Ishihara, K., & Furukawazono, K. (2000). Analysis of two case histories on liquefaction of reclaimed deposits. Proc. 12th World Conference on Earthquake Engineering, 1-10.
[9] Fenton, G. A., & Vanmarcke, E. H. (1998). Spatial variation in liquefaction risk. Geotechnique, 48(6), 819-831.
[10] Gianella, T., Stuedlein, A., & Canivan, G. (2015). Densification of liquefiable soils using driven timber piles. 6th Int. Conf. on Earthquake Geotechnical Engineering,
[11] Idriss, I. M., & Boulanger, R. W. (2008). Soil liquefaction during earthquakes Earthquake Engineering Research Institute.
[12] Ku, C., & Juang, C. H. (2011). Variation of CPTU parameters and liquefaction potential at a reclaimed land induced by dynamic compaction. Journal of GeoEngineering, 6(2), 89-98.
[13] Kulhawy, F. H., & Trautmann, C. H. (1996). Estimation of in-situ test uncertainty. Paper presented at the Uncertainty in the Geologic Environment: From Theory to Practice, 269-286.
[14] Li, C. C., Wang, Y. L., & Yuan, X. M. (2014). Research on regional dividing technology for liquefaction based on ArcGIS. Paper presented at the Applied Mechanics and Materials, 477 1109-1112.
[15] Montgomery, J., & Boulanger, R. W. (2016). Effects of spatial variability on liquefaction-induced settlement and lateral spreading. Journal of Geotechnical and Geoenvironmental Engineering, 143(1), 04016086.
[16] Phoon, K., & Kulhawy, F. H. (1999a). Characterization of geotechnical variability. Canadian Geotechnical Journal, 36(4), 612-624.
[17] Phoon, K., & Kulhawy, F. H. (1999b). Evaluation of geotechnical property variability. Canadian Geotechnical Journal, 36(4), 625-639.
[18] Pokhrel, R. M., Kuwano, J., & Tachibana, S. (2013). A kriging method of interpolation used to map liquefaction potential over alluvial ground. Engineering Geology, 152(1), 26-37.
[19] Popescu, R., Prevost, J., & Deodatis, G. (2004). 3D effects in seismic liquefaction of stochastically variable soil deposits.
[20] Popescu, R., Prévost, J. H., & Deodatis, G. (1997). Effects of spatial variability on soil liquefaction: Some design recommendations. Geotechnique, 47(5), 1019-1036.
[21] Rhyner, F. C.Densification of granular soils by pile driving and implications for evaluation of liquefaction. IFCEE 2018 (pp. 284-300)
[22] Robertson, P., & Wride, C. (1998). Evaluating cyclic liquefaction potential using the cone penetration test. Canadian Geotechnical Journal, 35(3), 442-459.
[23] Seed, B., & Lee, K. L. (1966). Liquefaction of saturated sands during cyclic loading. Journal of Soil Mechanics & Foundations Div, 92(ASCE# 4972 Proceeding)
[24] Seed, H. B., & Idriss, I. M. (1971). Simplified procedure for evaluating soil liquefaction potential. Journal of Soil Mechanics & Foundations Diisionv.
[25] Shen, M., Martin, J. R., Ku, C., & Lu, Y. (2018). A case study of the effect of dynamic compaction on liquefaction of reclaimed ground. Engineering Geology, 240, 48-61.
[26] Sun, C. (2012). Applications of a GIS-based geotechnical tool to assess spatial earthquake hazards in an urban area. Environmental Earth Sciences, 65(7), 1987-2001.
[27] Tanaka, Y. (1996). Liquefaction of reclaimed lands along osaka bay by great hanshin earthquake (1995.1. 17). The Sixth International Offshore and Polar Engineering Conference,
[28] Terzaghi, K., Peck, R. B., & Mesri, G. (1996). Soil mechanics in engineering practice John Wiley & Sons.
[29] Yasuda, S., Harada, K., Ishikawa, K., & Kanemaru, Y. (2012). Characteristics of liquefaction in tokyo bay area by the 2011 great east japan earthquake. Soils and Foundations, 52(5), 793-810.
[30] Youd, T. L., & Idriss, I. M. (2001). Liquefaction resistance of soils: Summary report from the 1996 NCEER and 1998 NCEER/NSF workshops on evaluation of liquefaction resistance of soils. Journal of Geotechnical and Geoenvironmental Engineering, 127(4), 297-313.
[31] Yu, M., Shieh, B., & Chung, Y. (2000). Liquefaction induced by chi-chi earthquake on reclaimed land in central taiwan. Sino-Geotech, 77, 39-50.